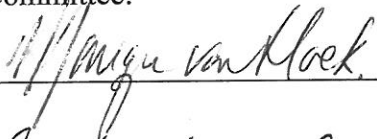


FRANCISELLA NOVICIDA INFECTION MODULATES THE MIRNA CONTENT IN
EXOSOMES RELEASED FROM MURINE MACROPHAGES.

by

Ryan Mackie
A Thesis
Submitted to the
Graduate Faculty
of
George Mason University
in Partial Fulfillment of
The Requirements for the Degree
of
Master of Science
Biology

Committee:



Dr. Monique L. van Hoek,
Thesis Director



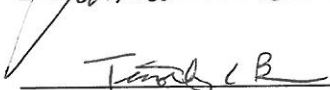
Dr. Geraldine Grant,
Committee Member



Dr. Kylene Kehn-Hall,
Committee Member



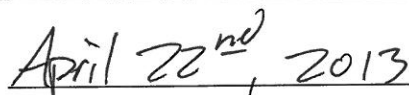
Dr. James D. Willett,
Director, School of Systems Biology



Dr. Timothy L. Born, Associate
Dean for Student and Academic Affairs,
College of Science



Dr. Vikas Chandhoke,
Dean, College of Science

Date: 

Spring Semester 2013
George Mason University
Fairfax, VA

Francisella novicida Infection Modulates the miRNA Content in Exosomes Released
from Murine Macrophages

A Thesis submitted in partial fulfillment of the requirements for the degree of Master of
Science at George Mason University

by

Ryan Mackie
Bachelor of Science
Colorado State University, 1999

Director: Monique L. van Hoek, Professor
School of Systems Biology

Spring Semester 2013
George Mason University
Fairfax, VA

Copyright: 2013 Ryan Mackie
All Rights Reserved

DEDICATION

This is dedicated to my Wife, Carrie, who is my fortress. Her commitments and sacrifices made it possible for me to pursue this long-sought achievement. Without her support and encouragement, the completion of this thesis would not have been possible.

This is also dedicated to my Father, Dr. William R. Mackie II, who drove me to success in this endeavor regardless of the distance between us or the increasing age with which I complete it. I will forever be thankful for his kind support and encouragement, and can only hope that I will find the strength of character to do the same for my children.

Finally, this is also dedicated to my Daughter, Olivia, and my Son, Reid. Stay in school as long as you can, for it is much harder to return once you have left.

ACKNOWLEDGEMENTS

I would like to thank my supervisor Dr. Monique L. van Hoek for her patience, support and direction during my graduate career. I would also like to thank my committee members, Dr. Geraldine Grant and Dr. Kylene Kehn-Hall, for their support of my research. I would like to thank Dr. Bradford Gutting at the Naval Surface Warfare Center, Dahlgren Division, for being a professional mentor and personal friend. I would also like to thank the Naval Surface Warfare Center in Dahlgren for their support through the Academic Fellowship Program. I would like to thank my lab members, Dr. Saira Ahmad, Dr. Myung Chul-Chung, Scott Dean, Moushimi Amaya, Nick Leverone, Stephanie Barksdale, Jessica Roman, Ekaterina Maraskova, Ravi Das and Liz Jaworski for helpful discussions, scientific scrutiny, and levity in times of need. Also, special thanks to Olivia Tiburzi, Dr. Peter Thielen and Dr. Chris Bradburne at The Johns Hopkins University Applied Physics Lab, for assistance with the miRNA sequencing efforts.

TABLE OF CONTENTS

| | Page |
|--|------|
| List of Tables | vi |
| List of Figures | vii |
| List of Abbreviations or Symbols | viii |
| Abstract | ix |
| Chapter One: Introduction | 1 |
| Chapter Two: Materials and Methods..... | 6 |
| Cell culture | 6 |
| Exosome-free Fetal Bovine Serum preparation | 6 |
| Exosome harvest and enrichment from naive cells | 7 |
| Characterization of exosomes | 7 |
| <i>Francisella</i> infection and LPS-treatment of J774A.1 macrophages for exosome harvest | 8 |
| RNA and protein extraction from harvested exosomes | 9 |
| Protein quantitation | 9 |
| Western Blot detection of exosomal proteins | 10 |
| cDNA preparation and RNASeq | 11 |
| qRT-PCR of miRNAs | 12 |
| Transfection of J774A.1 macrophages, infection with <i>F. Novicida</i> and determination of intracellular bacterial load and miRNA profiles | 13 |
| Chapter Three: Results..... | 15 |
| Exosome Characterization..... | 15 |
| Chapter Four: Discussion..... | 34 |
| References..... | 41 |

LIST OF TABLES

| Table | Page |
|--|------|
| Table 1: Agilent 2100 Bioanalyzer/small RNA and HS DNA Chip Results..... | 21 |
| Table 2: Top 25 Most Abundantly Expressed miRNAs | 25 |

LIST OF FIGURES

| | Page |
|---|------|
| Figure 1: DLS and SEM analysis of exosomes isolated from J774A.1 murine macrophages | 16 |
| Figure 2: Exosomes from <i>Francisella</i> infected murine macrophages contain CD63..... | 18 |
| Figure 3: Agilent 2100 Bioanalyzer analysis of micro and small RNAs libraries used for MiSeq sequencing runs | 20 |
| Figure 4: miR-155-5p and miR-146a-5p levels in naïve, <i>F. tularensis</i> LPS-treated, and <i>F. novicida</i> infected J774A.1 murine macrophages..... | 27 |
| Figure 5: miR-155-5p and miR-146a-5p levels in exosomes derived from naïve, <i>F. tularensis</i> LPS-treated, and <i>F. novicida</i> infected J774A.1 murine macrophages | 28 |
| Figure 6: miR-155-5p over-expression by pCMV-miR155 results in increased levels of miR-155-5p and miR-146a-5p measured by qRT-PCR | 30 |
| Figure 7: Intracellular levels of <i>F. novicida</i> is reduced in cells expressing higher levels of miR-155-5p and miR-146a-5p prior to infection | 31 |
| Figure 8: pCMV-miR155 transfected cells infected with <i>F. novicida</i> display higher levels of miR-155-5p and miR-146a-5p than non-transfected cells at 6 h post infection | 33 |

LIST OF ABBREVIATIONS

| | |
|-----------------------------|--------------------|
| LPS..... | Lipopolysaccharide |
| Ribonucleic Acid | RNA |
| Micro RNA | miRNA, miR |
| Small RNA..... | sRNA |
| Nucleotide..... | nt |
| Base Pair | bp |
| Multivesicular Bodies | MVBs |
| Intraluminal Vesicles | ILVs |
| Micrometer..... | μm |
| Nanometer..... | nm |
| Centipoise | cP |

ABSTRACT

Francisella novicida Infection Modulates the miRNA Content in Exosomes Released from Murine Macrophages

Ryan Mackie, MS.

George Mason University, 2013

Thesis Director: Monique L. van Hoek

Macrophages are the first line of innate defense for many diseases. Intercellular communication between infected macrophages and uninfected bystander cells of the host may be mediated via exosomes, small (50-100 nm) vesicles released from a variety of mammalian cell types shown to play a role in cell-cell communication and priming of the immune system. The contents of these extracellular vesicles include microRNA (miRNA) species that may represent a new mode of systemic signal transmission between either proximal or distal cells. We hypothesized that intracellular pathogens such as *Francisella* may affect the amount and type of RNA species that are predominantly packaged into exosomes compared to naïve, uninfected cells. We purified and characterized exosomes from *F. novicida* infected and uninfected J774A.1 murine macrophage cells. We analyzed the miRNA content of exosomes from infected cells by RNA sequencing and found differential miRNA expression contained therein. We demonstrate here that two murine miRNAs, miR-155-5p and miR-146a-5p, are up-regulated in infected cells and in the

exosomes released from these cells. We also demonstrate that delivery of exogenous miR-155-5p to naïve J774A.1 cells can alter their responsiveness to *F. novicida* infection and alter the cellular level of miR-146a-5p. Thus, exosomes from *Francisella* infected cells could deliver miRNAs to naïve bystander cells and alter their susceptibility to pathogen infection, and thus potentially modulate the host response to infection.

CHAPTER ONE: INTRODUCTION

Francisella tularensis subspecies *tularensis* is a Gram-negative facultative intracellular zoonotic pathogen and is the etiologic agent of the disease tularemia [1]. Fully virulent Type A strains of *Francisella* (e.g. SCHU S4) are pathogenic in humans, and it is thought that as few as ten bacteria are sufficient to cause pulmonary disease in humans. For this reason the CDC designates *F. tularensis tularensis* as a Category A Select Agent [2]. Other subspecies, including *F. tularensis novicida*, are less pathogenic in humans [3]. Although many of the cellular host-pathogen mechanisms associated with *Francisella* infection have been described, a complete understanding of the infection process remains to be defined, as do the determinants that dictate *Francisella* subspecies pathogenicity. Our interest is to begin to examine the role of macrophage-derived exosomes during *Francisella* infection and specifically, the potential role of microRNAs (miRNAs) in host-derived exosomes.

Exosomes are small membrane-derived vesicles that are released from a variety of mammalian cell types including macrophages and other immune cells. They are produced within intracellular structures called multivesicular bodies (MVBs) inside eukaryotic cells [4]. MVBs in turn contain intraluminal vesicles (ILVs). When MVBs fuse with the cytoplasmic cell membrane on the internal surface of the cell, they release ILVs as exosomes. The outer surface of an exosome is topographically equivalent to the outer

surface of the host cell membrane [5]. Exosomes range in size from 50-100 nm and often contain a large number of different membrane and cytoplasmic proteins which are specific to the cell type from which they originate [5, 6]. After release, circulating exosomes can fuse with neighboring cell membranes, become internalized, and release their luminal components into a neighboring cell. In this regard, exosomes can not only signal neighboring cells, but also deliver bioactive materials.

Exosomes contain various RNA species such as miRNAs. miRNAs can be transcribed either from an intronic sequence or as a part of a larger transcript containing a host gene mRNA. The larger primary miRNA (pri-miRNA) sequences may contain multiple miRNAs in as many as 70 nucleotides and are initially formed as stem-loop structures. Hairpin motifs contained in the pri-miRNA require post-transcriptional modification by the enzymes Drosha and DGCR8 in the nucleus of the cell prior to exportation. Processed miRNA are shuttled from the nucleus by association with Exportin-5 in an energy dependent process. Here they are further processed to mature miRNAs by the action of the RNase III enzyme Dicer. Mature miRNAs are 22-25 nucleotide (nt) non-coding RNAs which function in transcriptional gene regulation, mostly by base-pairing with messenger RNAs (mRNA). Often highly conserved in eukaryotic organisms, this mechanism of gene silencing is considered an evolutionary ancient form of translational repression that can aid in regulation of innate immune responses by a variety of cells. Finally, the incorporation of the mature miRNA in the RNA-induced silencing complex (RISC) with the target mRNA leads to repression or degradation.

During infection, *Francisella* bacteria are internalized by a variety of cell types and this process has been studied using several *in vitro* and *in vivo* systems. Generally, *Francisella* can escape the phagosomal compartment of phagocytes prior to fusion with lysosomes and proliferate in the cytoplasm of infected cells [7]. Alternatively, *Francisella* can invade non-phagocytic cell types by the interaction of bacterial ligands and host cell receptors in cell mediated processes such as macropinocytosis [8, 9]. Early endosomal compartments from epithelial cells that are infected by *Francisella* are degraded, and bacteria are capable of growth within the cytoplasm [8, 10]. A variety of bacterial attributes, including resistance to complement-based lysis and inhibition of cellular clearance by IFN γ -mediated activation of STAT1, have recently been discovered (Clay *et. al.*, 2008, Roth *et. al.*, 2009). Similar mechanisms aid the bacteria in escaping from the phagocytic compartment of monocytes and macrophages and promote bacterial survival [12]. Intracellular bacteria can then replicate in the cytosol and down-regulate pro-inflammatory cytokine production [13]. Cytokine signal inactivation, in part, allows bacterial proliferation to occur unchecked in the cytoplasm leading to apoptosis and bacterial escape.

Some mechanisms associated with cytokine down regulation have been worked out for different subspecies of *Francisella*. For example, during phagocytosis and compartmentalization of *F. novicida* into phagosomes, activation of the Toll-like Receptor 2/Myeloid differentiation primary response gene (88) (TLR2/MyD88) pathway leads to expression of cellular pro-inflammatory pathway constituents through the nuclear

factor kappa-light-chain-enhancer of activated B cells (NF- κ B) pathway [14]. Signaling through phosphoinositide-3-kinase (PI3K) in response to *F. novicida* infection serves to positively reinforce the NF- κ B transcription events and leads to signaling through Akt that reinforces the expression of other pro-inflammatory cytokines [12]. The phosphorylation of Akt by 3-phosphoinositide-dependent protein kinase-1 (PDK1) is dependent on the conversion of phosphatidylinositol 4,5-bisphosphate phosphatidylinositol to 3,4,5-trisphosphate (PIP3) by phosphoinositide-3-kinase (PI3K) [15, 16]. However, de-phosphorylation of PIP3 to Phosphatidylinositol 4,5-bisphosphate (PIP2) by Src homology 2-containing inositol phosphatase-1 (SHIP1) can preclude the downstream phosphorylation of Akt, thereby allowing SHIP1 to act as an antagonist of the cell survival pathway resulting from activated Akt [17]. Interestingly, the miRNA, miR-155-5p, has been shown to target the 3' untranslated region (UTR) of SHIP1 mRNA, down regulate its expression, and thus allow the phosphorylation of Akt and the cell survival pathway to proceed [18]. Furthermore, Cremer *et. al.* have recently demonstrated an increase in transcription of miR-155-5p in *F. novicida* infected cells, but not in response to fully virulent *F. tularensis* infection [19]. These observations suggest miR-155-5p may play a role in host-cell survival depending on which subspecies of *Franciseall tularensis* is used.

In addition to miR-155-5p, the regulatory role of another miRNA in adaptive and innate immunity, miR-146a-5p, has been previously described with respect to a variety of disease models and may play a role in *F. tularensis* infection. For example, targets for miR-146a-5p include Fas-associated death domain (FADD) [20], TRAF6 and IRAK1

[21], as well as IL-8 and RANTES [22]. Thus, through negative feedback control, miR-146a-5p could counteract the inflammation and cell-induced death pathways induced by TLR-2 receptor stimulation from *Francisella*-derived lipopolysaccharide (LPS). Additionally, miR-146a-5p has been reported to “fine-tune” levels of the pro-inflammatory cytokines such as TNF- α and IL-1 β , both of which are known to be critical in inhalational *Francisella* infections [23].

Thus, the aim of the current work was to begin to examine the potential role of exosomes and miRNAs during *Francisella* infection. Specifically, our hypothesis was that through miRNA delivery via exosomes, *F. novicida* infected macrophages may communicate their infected status and potentially affect innate immune response of naïve bystander cells. If supported, this may contribute to an increased understanding of the pathogenicity of *F. novicida*. Additionally, circulating exosomes containing miRNAs may represent potential biomarkers of *Francisella* infection, some of which may be specific to the subspecies of *Francisella* causing the infection.

CHAPTER TWO: MATERIALS AND METHODS

Cell culture

J774A.1 Murine macrophages were purchased from American Type Culture Collection (Cat # TIB-67, Manassas, VA) and maintained at 37°C/5% CO₂ in 0.22 µM-filtered Dulbecco's Modified Eagle's Medium (DMEM) amended with 10% Fetal Bovine Serum (Gibco). Periodic passage of the cells was accomplished by scraping cells from the tissue culture flask, centrifugation, and re-suspension in fresh medium. Cell counts were determined by hemocytometer, and cells were re-plated at 1.0 x 10⁶ cells per T75 flask. Fresh medium was added up to three times per week to maintain cell viability.

Exosome-free Fetal Bovine Serum preparation

Fetal Bovine Serum (FBS) used for exosome harvest experiments was either exosome-free as purchased from System Biosciences (Mountain View, CA) or was pretreated to remove existing serum exosomes prior to addition to cells in culture. Briefly, 28 ml aliquots of FBS were added to centrifuge tubes and weighed for balance. Tubes were centrifuged in the Sorvall JA ultracentrifuge at 110,000 x g for 2 h to form pellets of existing exosomes. Resulting supernatants were removed and pooled, and filtered using a 0.22 µm filter to remove any contaminants present in the centrifuge tubes. These portions of FBS were stored in 50 ml aliquots at -20°C until they were used. Exosome free serum was plated prior to the beginning of the exosome harvest experiments to ensure its sterility.

Exosome harvest and enrichment from naïve cells

T150 flasks containing 3.3×10^7 J774A.1 cells were maintained by routine culture methods for exosome harvest experiments. Maintenance cell culture medium was removed from all cell culture vessels by aspiration and cells were rinsed twice with sterile phosphate buffered saline (PBS) to remove trace contamination of serum-derived exosomes from growth medium. For naïve exosome production, 40 ml of cell culture medium containing exosome-free FBS was added to flasks, and flasks were incubated at 37°C/5% CO₂ for 72 h prior to removal of medium for exosome harvest. At 72 h, medium was removed from all cell culture flasks and filtered through 250 ml 0.22 µm filters prior to centrifugation. Filtered media was then aliquoted into ultracentrifuge tubes, weighed to ensure balance, and centrifuged at 10,000 x g at 4°C to remove cell debris. Resulting supernatants were removed to fresh ultracentrifuge tubes, balanced, and centrifuged at 100,000 x g at 4°C to pellet exosomes from culture media. Resulting supernatants were discarded, and pelleted exosomes were resuspended in 50µl of RNase A at 10ng/µl (Life Technologies, Grand Island, NY) and incubated for 10 min at 37°C to digest RNAs not contained within exosomes. The pellets were amended with 23 ml of ice-cold PBS, and centrifuged at 100,000 x g at 4°C to form final exosome pellets.

Characterization of exosomes

Prepared exosomes were diluted 1:1000 in 0.1M PBS, and incubated at 25°C prior to assay by Dynamic Light Scattering (DLS). Constant 25°C temperatures were maintained throughout the sampling procedure. Sampling frequency intervals were 4 µs and were run for a total of 200 s at a 90° angle of interrogation. Total particle counts were collected and measurements for size were compared across three independent runs to

generate the mean hydrodynamic diameter and standard error. The viscosity of the solution containing the exosomes was measured at 1.338 cP. The polydispersion indices for the replicates measured had a mean of 0.452 +/- 0.175 (SD) and was taken into account to determine accuracy of the distribution in unimodal read mode.

Exosomes in PBS were fixed by the addition of glutaraldehyde to a final concentration of 1.8% and incubated @ 4°C for 3 hours. Fixed exosomes were sputter coated with 2nm gold-palladium prior to viewing on the Hitachi SU8000 Scanning Electron Microscope (SEM). Images resolved were processed using the manufacturer's software.

***Francisella* infection and LPS-treatment of J774A.1 macrophages for exosome harvest**

T150 flasks containing 3.3×10^7 J774A.1 cells were maintained as above. Upon removal of maintenance media, 40 ml of cell culture medium containing fresh culture aliquots of *Francisella novicida* (BEI NR-13) at an MOI of 50 or 100 $\mu\text{g/ml}$ *F. tularensis* LVS LPS (BEI NR-2627) were added to the culture vessels (n=4) at t=0. Live bacteria and LPS were allowed to incubate in the presence of J774A.1 macrophages for 2 h at 37°C and 5% CO₂ before aspirating the media. At t=2 h, cells were rinsed three times to physically remove extracellular bacteria or LPS, and infected cells were treated with media containing 50 $\mu\text{g/ml}$ Gentamicin for 1 hour to kill adherent extracellular bacteria. Infected cells were rinsed once more with cell culture medium containing exosome-free FBS, and incubated for 72 h with medium containing 2 $\mu\text{g/ml}$ gentamicin to prevent further bacterial growth. At 72 h p.i., exosomes were harvested as above.

RNA and protein extraction from harvested exosomes

Exosomes harvested from cell culture medium were washed in ice-cold PBS, as above, and re-suspended in 500 μ l of Disruption Buffer containing 2-mercaptoethanol from the miRVANA PARIS protein and RNA isolation system (Ambion, Carlsbad, CA). 200 μ l of Disruption Buffer from the exosomal pellet was removed from each sample, stored on ice for 5 min, and transferred to a fresh tube and stored as the protein fraction. The remainder of the Disruption Buffer (300 μ l) was amended with 300 μ l of 2X Denaturation buffer, mixed by vortex and allowed to incubate for 5 min on ice. 600 μ l of cold Acid-Phenol:Chloroform (24:1) was added to each sample extracted and vortexed to mix. Samples were centrifuged at 10,000 x g for 5 min at RT and the aqueous phase containing total RNA was removed to a fresh tube. Ethanol was added to each sample and mixed by inversion. The ethanol/aqueous portions were added to the glass fiber filters washed once with wash buffers. Filters were placed into fresh collection tubes and 100 μ l of elution buffer was added to each sample. Tubes containing RNA bound to filters were centrifuged @ 5,000 x g for 2 min to collect RNA, and stored at -80°C until processed.

Protein quantitation

Protein isolated using the mirVANA PARIS kit was quantified by bicinchoninic acid assay (BCA) (Pierce, Rockford, IL). Protein samples isolated from the exosomal pellets were diluted 1:10, 1:25 and 1:100 in sterile PBS prior to assaying. Protein supplied by the manufacturer (Bovine Serum Albumin) was used to create a standard curve with a range of 25 – 2,000 μ g/ml. Unknown protein concentration from the samples were determined by mixing 25 μ l of each diluted protein sample and protein standard

(n=3) with 200 μ l of working reagent (50:1, Reagent A:B) in a microplate assay. Plates were allowed to shake for 30 sec at RT and incubated at 37°C for 30 minutes. After incubation, plates were cooled to RT and absorbances for each well were recorded at 562 nm on the μ Quant plate reader (BioTek, Winooski, VT).

Western Blot detection of exosomal proteins

Separation of cellular and exosomal proteins was accomplished by two methods. Native polyacrylamide gels were used to separate non-reduced proteins for use in Western blotting assays using an anti-CD63 antibody (Abcam, Cambridge, MA) which recognizes the native epitope. Additionally, we separated proteins using 4-12% Bis-Tris gels (Novex) after denaturing the protein samples in 4X Laemmli buffer treated to 95°C for 5 min. Denatured proteins were probed using a different anti-CD63 antibody (Santa Cruz Biotech, Santa Cruz, CA). Similar protein amounts were added to the lanes of the polyacrylamide gels. After separation, the proteins were transferred to PVDF membranes using the Invitrogen iBlot system (Grand Island, NY) using the 125 milliamps for 7 minutes. Blocking of the membrane occurred in 1% non-fat milk in Tris-buffered saline containing 0.1% Tween-20. After blocking, both antibodies were added to the blocking solution at manufacture recommended concentrations and allowed to incubate overnight with agitation at 4°C. After incubation, blots were washed 3 times with TBS-T with gentle agitation for 15 min at Room Temp. Polyclonal secondary antibodies (Rabbit anti-Mouse) were added to TBS-T at 1:15,000 dilutions and allowed to incubate at RT for 2 h with gentle agitation. Once again, blots were washed with TBS-T 3 times at RT with gentle agitation. Finally, the blots were removed from the secondary antibody incubation

and overlaid with Pierce West Femto chemiluminescent detection reagent and imaged with the BioRad ChemiDoc XRS + system (Hercules, CA).

cDNA preparation and RNASeq

miRNA samples obtained from the extraction procedure above were quantified using the Agilent 2100 bioanalyzer, and diluted to meet the manufacturer's recommendations for RNA input to the TruSeq small RNA sample preparation. The amount of RNA used in the TruSeq small RNA preparation process was equivalent to what would normally be assumed from 10 µg of total RNA (1 µg). Ligation of 3' and 5' adapter sequences were accomplished using T4 RNA Ligase 2 and T4 RNA Ligase in separate reactions, respectively. Reverse transcription and amplification of ligated products was carried out in the presence of the RNA RT primer and the RNA PCR primer indices, respectively, in order to create the cDNAs and to index and separate the samples once pooled. PCR amplification strategy followed the manufacturer's instructions and included a thermal cycler profile of 98°C for 30 seconds followed by 11 cycles of 98°C for 10 sec / 60° for 30 sec / and 72°C for 15 sec, followed by a 4°C hold.

Products were evaluated once more on the Agilent 2100 Bioanalyzer using the high sensitivity DNA chip. Separation of the cDNA constructs on 6% PAGE Gels was carried out in 1x TBE with the High Resolution Ladder and 1 µl of DNA Loading Dye (Illumina). Gels were run for 60 minutes at 145 V until the dye front exited the bottom of the gel. Gel slices containing the bands of interest were excised from the gel with a sterile scalpel and were broken using Gel Breaker tubes (IST Engineering, Milpitas, CA).

Recovery and precipitation of the amplified cDNAs was performed using molecular grade water followed by ethanol precipitation with glycogen and 3M Sodium acetate.

The instrument protocol followed to perform the RNA sequencing was the Illumina 15012197 Rev.D for library preparation and sequencing. The 50bp MiSeq v2 cartridge (cat# MS-102-2001) was used for the small RNA range of size-selected samples, and a second run using the 2x150 v2 cartridge (cat# MS-102-2002) was performed in order to sequence the larger fragments. After pooling for size selection, the libraries were run on the Agilent 2100 Bioanalyzer using the High Sensitivity DNA chip (cat# 5067-4626) and further quantified with Picogreen (Invitrogen Quant-IT, cat# P11496) and finally with the Kapa Library Quantification kit for Illumina (cat# KK4835). The MiSeq flow cell was loaded at 10pM for each sequencing run.

qRT-PCR of miRNAs

miRNA fractions isolated using the *MirVana* kit above served as the template for the subsequent reverse transcription reactions followed by relatively quantitative polymerase chain reactions (qRT-PCR). The universal cDNA synthesis kit from Exiqon (Woburn, MA) was used to poly-adenylate and reverse transcribe the miRNAs isolated from naïve and exosomes from infected cells in 10 µl single-step reactions. RT reactions were incubated @ 42°C for one hour to complete the cDNA synthesis, and resulting templates were diluted 20X in order to serve as the template for multiple real-time PCR reactions. Multiple aliquots of 2X PCR master mix containing SYBR Green (Bio-Rad, Hercules, CA) were mixed with equivalent volumes of miRCURY LNA® primers purchased from Exiqon. Primers for murine miR-155-5p (Cat#205080, Exiqon), miR-

146a-5p (Cat#204401, Exiqon) and U6b snRNA (Cat#203450, Exiqon) were used to amplify the corresponding cDNA sequences from all samples, and U6 snRNA signals were used to calibrate the relative expression of miR-155-5p and miR-146a-5p. Relative quantitation values, using the naïve or untreated cells as calibrators, and statistical measures used to determine the significance of the assay results were obtained using the qPCR instrument software (BioRad CFX manager V 3.0, Hercules, CA). Separate stand-alone software (Kyplot, Tokyo) was used to perform descriptive statistics.

Transfection of J774A.1 macrophages, infection with *F. Novicida* and determination of intracellular bacterial load and miRNA profiles

Macrophages were seeded in each well of a 24-well plate (1×10^5 cells/well) (Corning, NY) in Dulbecco's Modified Essential Medium amended with 10% FBS and incubated overnight at 37°C and 5% CO₂. Twenty-four hours after seeding, cell media was amended with 50 µl of OptiMEM (Gibco) containing Avalanche J774A.1 transfection reagent (EZBiosystems, College Park, MD) alone, or in combination with 1.5 µg pCMV control vector (empty) or 1.5 µg pCMV-miR155 (OriGene, Rockville, MD). Cells were allowed to rest for 24 h to induce miR-155-5p expression from the vector containing the insert. At 24 h, cells were analyzed for transfection efficiency by monitoring GFP expression included in the vector construct and under the control of the IRES-GFP cassette. Transfection efficiency for each well was calculated by direct count, and approached 50% (data not shown). Duplicate wells were lysed, and miRNA was isolated using the mirVANA PARIS kit as above to determine miR-155-5p and miR-146a-5p expression before commencement of the infection. Transfected cells were infected the same as above, and were allowed to incubate for a total of 6 h p.i. Infected

cells were rinsed twice with PBS to remove gentamicin and lysed by the addition of 0.2% SDS in pure water. Lysis was quick and complete, and lysates were immediately amended with 10X PBS to avoid bacterial lysis. Serial dilution in 1XPBS and plating of each well on Trypticase-Soy agar plates containing 0.1% L-cysteine followed by incubation for 36 h at 37°C was carried out to determine the intracellular bacterial burden. miRNA was isolated from duplicate t=6 hour wells where cells were not lysed by SDS. All miRNA samples were measured by Nanodrop UV/VIS spectrophotometer (Thermo, Wilmington, DE) and adjusted to 5 ng/μl. cDNA creation was carried out as above and qRT-PCR was performed with miR-155-5p and miR-146a-5p primers from Exiqon (Woburn, MA) as above.

CHAPTER THREE: RESULTS

Exosome Characterization

Exosomes isolated from uninfected J774A.1 cell culture medium were characterized by DLS and SEM to determine size distribution (**Figure 1A**). The average particle count/ml determined by DLS was 1.67×10^5 /ml. Consistent with DLS experiments by others, the exosomes had a mean diameter of 202.80 ± 10.95 nm (mean \pm SEM) and a polydispersion index that ranged from 0.215 - 0.633 in three separate replicates [25]. Employing the filtration and differential centrifugation technique to harvest the macrophages from the culture media led to large clumps of exosomes. The PI value from the DLS analysis supports a higher mean hydrodynamic diameter and suggested the exosomes were not monodisperse. This result was confirmed by SEM imaging where multiple small groups of exosomes were visualized (**Figure 1B**).

A

| Rept.# | Mean (nm) | P.I. | Diff.Coeff (m ² /s) | Counts/s | Baseline Error | Overflow |
|---------|---------------|---------------|--------------------------------|----------|----------------|----------|
| Rept.1 | 213.0 | 0.215 | 2.28e-12 | 1.69e+05 | 0.10% | 0 |
| Rept.2 | 207.8 | 0.509 | 2.33e-12 | 1.67e+05 | 0.12% | 0 |
| Rept.3 | 187.5 | 0.633 | 2.58e-12 | 1.68e+05 | 0.09% | 0 |
| Average | 202.8 ± 10.98 | 0.452 ± 0.175 | | | | |

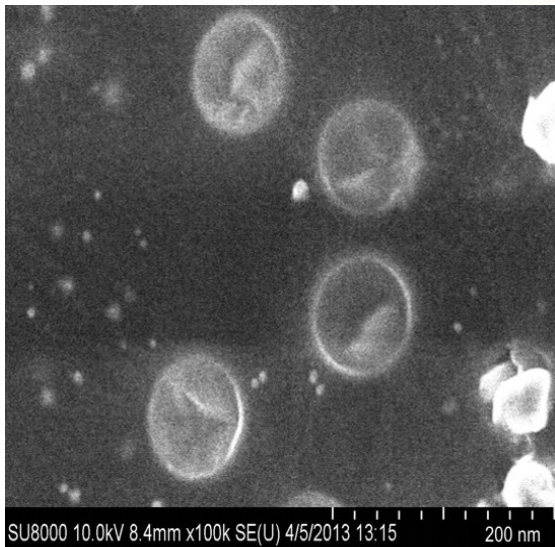
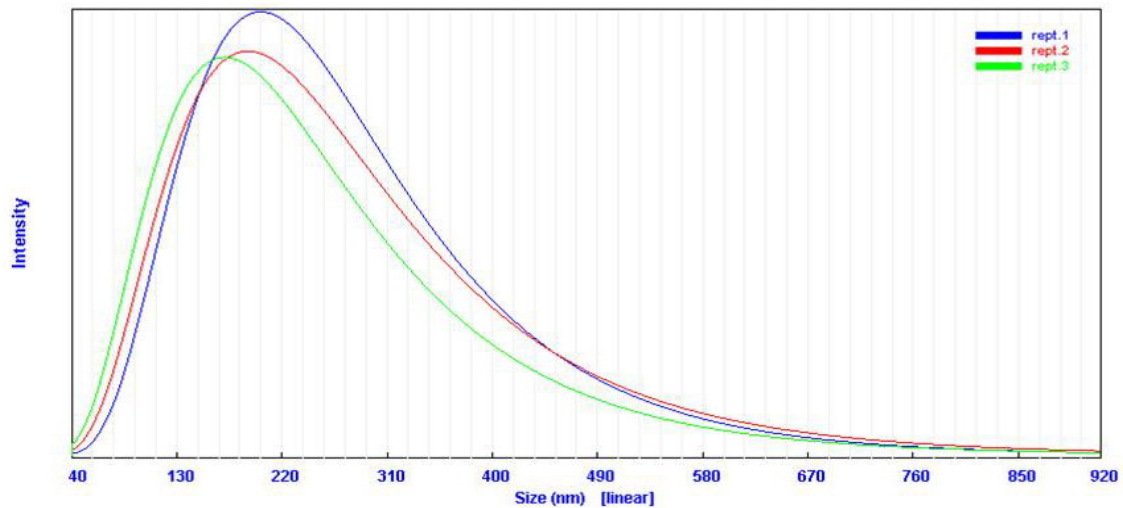
**B**

Figure 1. DLS and SEM Analysis of Exosomes Isolated from J774A.1 Murine Macrophages. (A) Exosome diameter (mean diameter \pm SD; n=3) was 202.8 ± 10.96 nm as determined by Dynamic Light Scattering (DLS). DLS Polydispersity indices (PI) of 0.215 – 0.633 suggested exosomes were not monodisperse, but existed in small, tightly packed groups. This was confirmed by SEM where multiple exosome images showed 4-8 exosomes per group (B).

CD63, a tetraspanin-family glycoprotein with a molecular weight of ~ 53 kDa, is commonly used as a marker of exosomes [30]. CD63 was present in exosomes from naïve and infected cells at the expected molecular weight (**Figure 2**) [31]. Here, CD63 was probed using two different CD63-specific antibodies, one which recognized the native form of CD63 and the other recognized the denatured form. The two different antibodies were used because the samples were generated using the mirVANA PARIS isolation kit. Using this kit, the sample is reduced by the presence of β -mercaptoethanol during the preparation of the RNA and protein from the same sample. Collectively, separation on two different gel types and Western Blot analysis using two different antibodies, together with the size data from the SEM analysis, ensured that the population of microvesicles were exosomes.

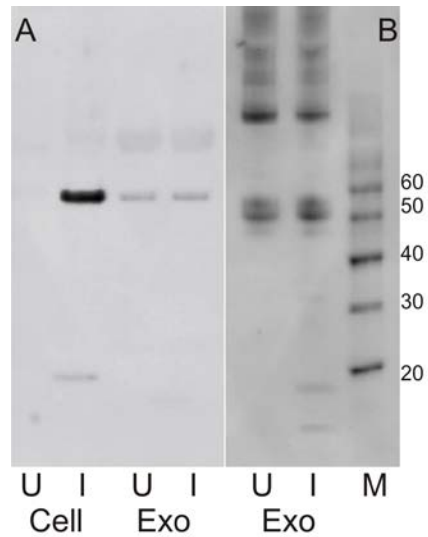


Figure 2. Exosomes from Fn infected murine macrophages contain CD63, an exosome marker protein. (A) Proteins from naïve (U) and *Francisella* infected (I) J774A.1 Murine macrophages (cell) and exosomes harvested from the cell culture media (Exo) were separated on NativePAGE Bis-Tris gels (Novex) and transferred by Western Blot. Blots were probed with anti-CD63 antibodies that recognize the non-denatured proteins (Abcam). (B) Denatured exosomal proteins were also separated by 4-12% Bis-Tris PAGE gels and transferred by Western blot. Blots were probed with anti-CD63 antibodies that recognize the reduced CD63 protein. Marker (M) indicates the approximate protein molecular weight in KDa.

RNA purification and quantitation

RNA samples isolated from naïve and *Francisella*-infected cells, as well as from harvested exosomes, were characterized using the Agilent 2100 Bioanalyzer and the small RNA microfluidic chip. Gel lanes for the cellular and exosomal RNAs showed varied intensity bands in the 20-40 nucleotide range (**Figure 3A**), which is consistent with miRNAs derived from host cells and exosomes. Bands in the 41-60 nucleotide range represented transfer RNAs and others species, whereas RNAs larger than 60 nucleotides represented other sRNAs. In an additional step, the acid phenol:chloroform and glass-fiber filters present in the mirVANA kit allowed further enrichment for small and miRNA species with the addition of small volumes of 100% ethanol to remove larger RNA species and subsequent isolation of smaller RNAs with additional ethanol [32]. As a result, the average size for the miRNAs extracted from exosome and cellular samples ranged from 28-30 nucleotides while the average size of sRNAs isolated from the samples ranged from 51-102 nucleotides. When quantified, concentrations for the exosome and cellular miRNAs ranged from 3.7-11.8 ng/ml and 28-984 ng/ml, respectively (**Table 1**). The sRNA species (> 40 nt) isolated from the same samples ranged from 12-35.5 ng/ul for exosomes and 455.5-1248.7 ng/ml for cells. There are some visible differences in the gel banding patterns in exosomes from infected cells (Lane 3) as compared to the naïve or LPS-treated (Lanes 1 and 2, respectively). These data aided sequencing efforts by helping to normalize the amount of starting material for the Illumina TruSeq Small RNA sample preparation kit (see below).

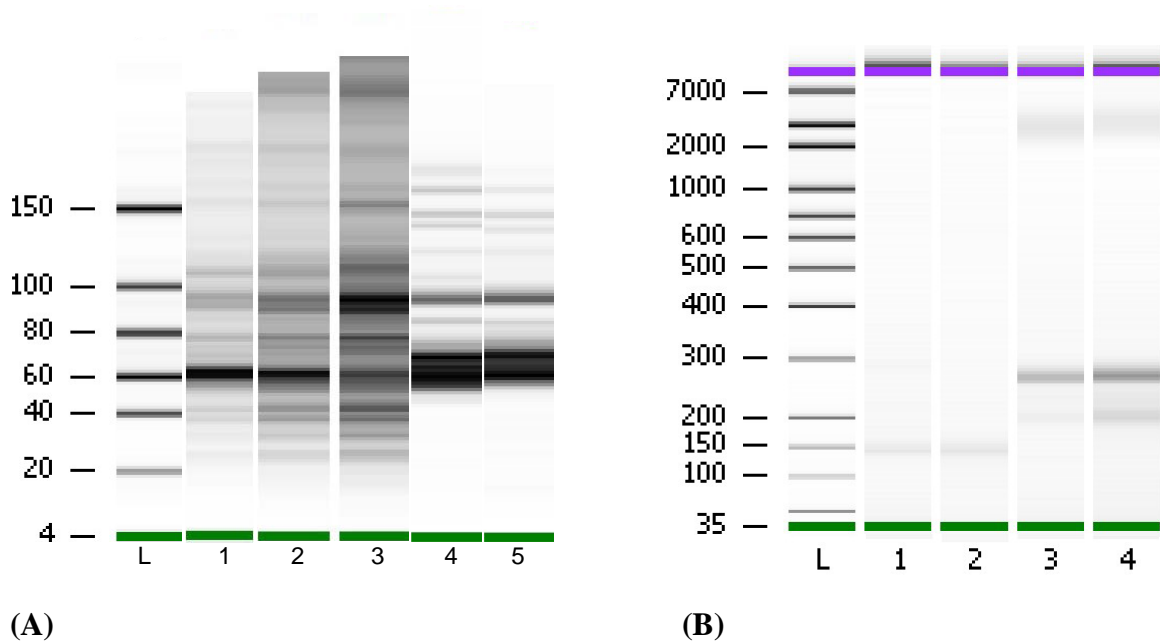


Figure 3. Agilent 2100 Bioanalyzer analysis of micro and small RNAs libraries used for MiSeq sequencing runs. (A) RNA samples isolated from exosomes and cells. Naïve, LPS-treated and exosomes from infected cells (lanes 1, 2, and 3) show similar patterns of miRNA and sRNA banding with increased intensity in the miRNA region (20-40 nt) in exosomes from infected cells. Cellular RNA isolates are enriched in tRNAs (~60nt) and other sRNA species (lanes 4 and 5). **(B)** The Agilent 2100 Bioanalyzer High-Sensitivity DNA chip was used to characterize the libraries of the reverse transcribed miRNA and sRNA species. Bands between 125 and 150 represent the miRNA population (lanes 1 and 2) and bands between 200 and 300 represent sRNAs (lanes 3 and 4). Lanes marked L denotes the ladder and size in nucleotides is listed.

| | | |
|-----------------------|--------------------------|-------------------------------------|
| Naive exosomes | Average Size [nt] | Conc. [pg/μl] |
| miRNA | 29 | 3,775.70 |
| Small RNA | 79 | 12,013.10 |
| Fn + exosomes | Average Size [nt] | Conc. [pg/μl] |
| miRNA | 30 | 11,862.10 |
| Small RNA | 102 | 35,548.50 |
| LPS + exosomes | Average Size [nt] | Conc. [pg/μl] |
| miRNA | 30 | 9,353.70 |
| Small RNA | 95 | 25,269.90 |
| <hr/> | | |
| Naive Cell | Average Size [nt] | Conc. [pg/μl] |
| miRNA | 28 | 28,206.20 |
| Small RNA | 46 | 45,539.30 |
| Fn + Cell | Average Size [nt] | Conc. [pg/μl] |
| miRNA | 28 | 984,305.90 |
| Small RNA | 55 | 1,248,742.00 |
| LPS + Cell | Average Size [nt] | Conc. [pg/μl] |
| miRNA | 30 | 432,413.40 |
| Small RNA | 51 | 673,603.80 |

Table 1: Agilent 2100 Bioanalyzer/small RNA Chip Results for sRNA and miRNA isolated from Cells and Exosomes.

miRNA sequencing reveals various miRNAs are modulated between uninfected and infected cells and exosomes

In order to determine changes to the miRNA population in response to *Francisella* infection, sequencing experiments were conducted using the Illumina MiSeq on exosomes from naïve, LPS-treated and *Francisella* infected cells. Initially, all RNA species < 200 nt, including miRNAs, were sequenced in one run using the 2x150 bp MiSeq v2.0 cartridge. The library creation strategy employed a size exclusion step that allowed separation of the miRNA subpopulation from other sRNAs. Here, a cutoff size for each run created subsamples of the amplified library as they were excised from the gel purification step. Analysis showed that two sub-populations were created from the initial total RNA isolation (**Figure 3B**). The miRNA population was then sequenced using the TruSeq Small RNA kit and the 50bp MiSeq v2.0 cartridge in order to capture a broad picture of the very small transcripts present in all sample types.

The sequencing results are shown in **Table 2**. The results are heat-map colored to highlight the difference between miRNA transcripts identified among sample types and Table 2 also shows the 25 most abundantly detected transcripts for the respective sample. The level of relative expression is ranked in each treatment group with the highest expressed transcript at the top. When comparing the difference between two sample types, transcripts highlighted in green denote transcripts with similar abundance between the two groups and yellow highlighted transcripts indicate a large difference in relative abundance between the sample types. Red highlighted transcripts indicate the transcript is present only in the top 25 most abundantly detected transcripts in that sample. By presenting results this way, data could be examined across treatment and sample type, as

well as abundance. As shown, several of the miRNAs were detected in all sample types. For example, miR-27b-3p was present in all samples and also appeared to be the most abundantly sequenced miRNA across all sample types. In contrast, miR-301a-5p, miR301b-5p and miR-103-1 were not detected in infected cells while some transcripts were present only in infected cells - miR-30a-5p, miR-146b-5p and miR-101a. Finally, with respect to exosomes from infected cells, 3 miRNAs (miR-3074-1-5p, miR-3074-2-5p and miR-192-5p) were detected only in exosomes harvested from infected cells.

The data also suggest that while some miRNA species were identified in all samples, a variety of them were appeared to be differentially packaged in the exosome samples under certain experimental conditions. For example, miR-186-5p, miR-135a-5p and miR-146b-5p appeared with high relative abundance in exosomes from infected cells but were not detected in exosomes from naïve cells. Similarly, miR-186-5p, miR-221-5p and miR-26a-5p were detected in exosomes from cells treated with *F. tularensis* LVS LPS, but not in exosomes from naïve cells. Conversely, the exosomes from infected cells did not contain miRNAs found in relatively high abundance in naïve exosomes, such as miR-let-7f-5p, miR-let-7d-3p nor miR-let-7c-5p, among others. These results suggest that the difference between miRNAs identified from infected vs. naïve exosomes can be attributed to both the increased packaging of some transcripts and the decreased packaging of others with respect to sample type.

Because miR-155-5p plays an important role in *F. novicida* infection [19], it was of interest to examine this miRNA closer. miR-155-5p was not identified as one of the top 25 miRNA transcripts in exosome or cellular samples, but was identified in relatively

low abundance in naïve samples and higher abundance in infected samples (**Table 2**). The ratios of the normalized abundance for all mapped transcripts for miR-155-5p were detected approximately 4:1 (0.267 infected vs 0.066 naïve) in exosome samples and 20:1 (0.119 infected vs. 0.0061) cellular samples. The average number of sequencing hits from infected cells and exosomes for miR-155-5p was 2.3×10^3 and 1.4×10^2 respectively.

Finally, miR-146a-5p was detected in relatively high abundance in all sample types, and was ranked as the 7th and 8th most abundantly sequenced transcript in exosomes and infected cells, respectively. This was a significant increase in abundance in comparison to the naïve exosome and cellular samples. Interestingly, miRNA-146, and its pri-miRNA relative miRNA-146b, were absent in the Top 25 list from *Francisella* LPS treated exosomes and from *Francisella* LPS treated cells, although they appeared to be constitutively expressed in naïve cells and exosomes. Sequencing results demonstrated that miR-146a-5p was ubiquitously expressed in infected sample types with an average number of 2.5×10^4 and 6.1×10^3 for cell and exosomes, respectively.

Table 2: Top 25 Most Abundantly Expressed miRNAs from Naïve cells and infected cells, and from exosomes harvested from naive, LPS-treated, *F. novicida* infected cells.

| Naïve Cell | Fn Infected Cell | Naïve Exosome | LPS + Exosome | Naïve Exosome | Fn Infected Exosome |
|---------------|------------------|---------------|---------------|---------------|---------------------|
| miR-27b-3p | miR-27b-3p | miR-27b-3p | miR-27b-3p | miR-27b-3p | miR-27b-3p |
| miR-191-5p | miR-21a-5p | miR-3107-5p | miR-3107-5p | miR-3107-5p | miR-22-3p |
| miR-22-3p | miR-22-3p | miR-22-3p | miR-22-3p | miR-22-3p | miR-191-5p |
| miR-99b-5p | miR-191-5p | miR-191-5p | miR-92a-3p | miR-191-5p | miR-3107-5p |
| miR-301a-3p | miR-99b-5p | miR-21a-5p | miR-21a-5p | miR-21a-5p | miR-21a-5p |
| miR-21a-5p | miR-10a-5p | miR-10a-5p | miR-191-5p | miR-10a-5p | miR-30a-5p |
| miR-10a-5p | miR-30a-5p | miR-92a-3p | miR-10a-5p | miR-92a-3p | miR-146a-5p |
| miR-148a-3p | miR-146a-5p | miR-99b-5p | miR-142-3p | miR-99b-5p | miR-16-5p |
| miR-16-5p | miR-142-3p | miR-142-3p | miR-148a-3p | miR-142-3p | miR-99b-5p |
| miR-3107-5p | miR-3107-5p | miR-423-3p | miR-25-3p | miR-423-3p | miR-10a-5p |
| miR-142-3p | miR-16-5p | miR-16-5p | miR-16-5p | miR-16-5p | miR-142-3p |
| miR-146a-5p | miR-146b-5p | miR-148a-3p | miR-99b-5p | miR-148a-3p | miR-181a-5p |
| miR-92a-3p | miR-148a-3p | miR-615-3p | miR-let-7f-5p | miR-615-3p | miR-30d-5p |
| miR-let-7f-5p | miR-181a-5p | miR-30d-5p | miR-let7i-5p | miR-30d-5p | miR-92a-3p |
| miR-181a-5p | miR-125a-5p | miR-222-3p | miR-423-3p | miR-222-3p | miR-186-5p |
| miR-let-7c-5p | miR-186-5p | miR-25-3p | miR-let-7c-5p | miR-25-3p | miR-125a-5p |
| miR-let7i-5p | miR-222-3p | miR-let-7f-5p | miR-30a-5p | miR-let-7f-5p | miR-222-3p |
| miR-351-5p | miR-92a-3p | miR-146a-5p | miR-181a-5p | miR-146a-5p | miR-148a-3p |
| miR-30d-5p | miR-let-7c-5p | miR-181a-5p | miR-10b-5p | miR-181a-5p | miR-192-5p |
| miR-25-3p | miR-let-7f-5p | miR-let7d-3p | miR-451a | miR-let7d-3p | miR-3074-2-5p |
| miR-186-5p | miR-let7i-5p | miR-let-7c-5p | miR-101a-3p | miR-let-7c-5p | miR-301a-3p |
| miR-222-3p | miR-30d-5p | miR-10b-5p | miR-186-5p | miR-10b-5p | miR-210-3p |
| miR-125a-5p | miR-25-3p | miR-30a-5p | miR-221-5p | miR-30a-5p | miR-3074-1-5p |
| miR-301b-3p | miR-351-5p | miR-210-3p | miR-222-3p | miR-210-3p | miR-146b-5p |
| miR103-3p | miR-101a-3p | miR-101a-3p | miR-26a-5p | miR-101a-3p | miR-25-3p |
| | | | | | |
| miR-155-5p | miR-155-5p | miR-155-5p | miR-155-5p | miR-155-5p | miR-155-5p |

Note: The level of relative expression is ranked in each treatment group with the highest expressed transcript at the top. When comparing the difference between two sample types, transcripts highlighted in green denote transcripts with similar abundance between the two groups and yellow highlighted transcripts indicate a large difference in relative abundance between the sample types. Red highlighted transcripts indicate the transcript is present only in that sample.

qRT-PCR to validate the miRNA profiles from uninfected vs. Infected exosomes

Expression levels of specific miRNA species of interest were further examined using the Exiqon universal cDNA synthesis kit followed by specific miRNA LNA primers for miR-155-5p and miR-146a-5p from infected and uninfected cells, as well as exosomes from both cell-treatment types.

At 72 hours post-infection, miR-155-5p levels in *F. novicida* infected cells vs. naïve cells were 29.6-fold (+/- 10.72 SEM) higher, supporting the relative difference seen by RNASeq data (**Figure 4**). This suggested *F. novicida* infection in murine macrophages leads to an increased cellular levels of miR-155-5p, which is consistent with previous observation [19]. In addition, the miR-155-5p level in the exosomes derived from *F. novicida* infected cells were 1.8-fold (+/- 0.37 SEM) higher than exosomes derived from naïve cells (**Figure 5**). miR-155-5p levels in cells and exosomes treated with LPS from *F. tularensis* LVS were not significantly increased compared to naïve samples (**Figure 4 and 5**).

Similarly, miR-146a-5p levels were 14.54-fold (+/- 4.93 SEM) higher in infected cells vs. non-infected cells, supporting the relative difference seen in the RNASeq data (**Figure 4**), which to our knowledge has not been previously reported for *F. novicida* infection in this cell type. Furthermore, miR-146a-5p was 2.9-fold (+/- 0.63 SEM) higher in exosomes from infected cells compared to naïve exosomes (**Figure 5**). miR-146a-5p levels in cells and exosomes treated with LPS from *F. tularensis* LVS were not significantly increased compared to naïve samples, which was not in line with data from RNASeq (**Figure 4 and 5**).

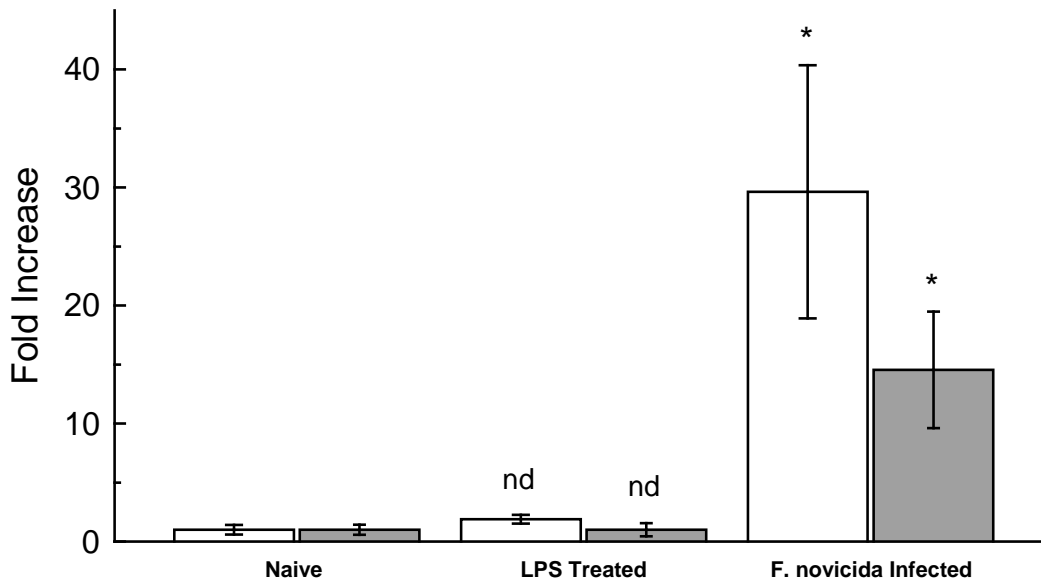


Figure 4. miR-155-5p and miR-146a-5p Levels in Naïve, *F. tularensis* LPS-treated, and *F. novicida* infected J774A.1 Murine Macrophages. A 29.6-fold increase in miR-155-5p (white bars) and 14.5-fold increase in miR-146a-5p (grey bars) isolated from J774A.1 macrophages harvested at t=72 hours p.i with *Francisella novicida*. No significant increase seen in macrophages treated with *Francisella* LPS treated (100ng/ μ l) cells. n=5 for all groups. # indicates significant increase (p -value < 0.05) by Student's t-test. nd indicates no significant difference compared to control. Error bars are standard error of the mean of fold change.

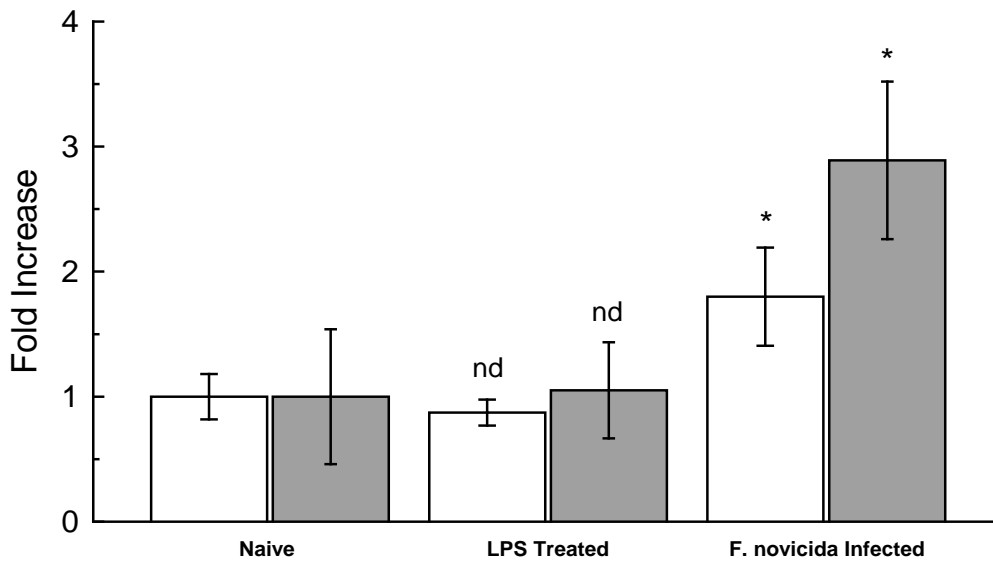


Figure 5. miR-155-5p and miR-146a-5p Levels in Exosomes Derived from Naïve, *F. tularensis* LPS-treated, and *F. novicida* infected J774A.1 Murine Macrophages. A 1.79 +/- 0.39-fold increase in miR-155-5p (white bars) and 2.89 +/- 0.63-fold increase in miR-146a-5p (grey bars) in exosomes harvested at 72 h p.i from *F. novicida*. No significant increase in these miRNA species was detected from exosomes derived from *Francisella* LPS-treated (100ng/μl) cells. n=5 for all groups. * indicates significant change (p -value < 0.05) by Student's t-test. nd indicates no significant difference compared to control. Error bars are standard error of the mean of fold change.

Reduced bacterial load in cells expressing higher levels of miR-155-5p

After confirmation of the specific miRNA content in infected cells and exosomes by qRT-PCR, experiments were designed to better understand the biological significance of miR-155-5p overexpression in this cell infection model. We aimed to simulate a condition where exosomes with elevated levels of miRNAs released from infected cells could be taken up by neighboring uninfected, naïve bystander cells. Here, the OriGene pCMV-MIR vector was used to transfect J774A.1 cells at a cell density of 1×10^5 per well. The level of miR-155-5p or miR-146a-5p was measured by qRT-PCR 24 hours post-transfection. A 21.9-fold (\pm 9.4 SEM) increase in the level of miR-155-5p was detected in transfected cells when compared to empty vector-transfected or naïve cells using the U6B snoRNA as a reference gene (**Figure 6**) and there was also a 10.3-fold (\pm 1.7 SEM) increase in miR-146a-5p at 24 h in the pCMV-155 transfected cells. These results were determined by comparison with empty pCMV vector and both were statistically significant by Student's t-test ($p < 0.05$).

All groups of transfected cells were subsequently infected with *F. novicida* at an MOI of 50. After 6 h, pCMV-155 transfected cells demonstrated a 73.8% decrease in intracellular bacteria compared to cells transfected with the empty vector and a 77.4% decrease when compared to naïve cells (p -value < 0.01). Total intracellular bacterial levels in pCMV-miR155 transfected cells at 6 hours were 9,300 \pm 1,800 (mean + SEM) per well, whereas for non-transfected cells, the total intracellular burden was 41,000 \pm 5,000 (**Figure 7**). No significant difference was observed between naïve and vector-only transfected cells ($p=0.29$).

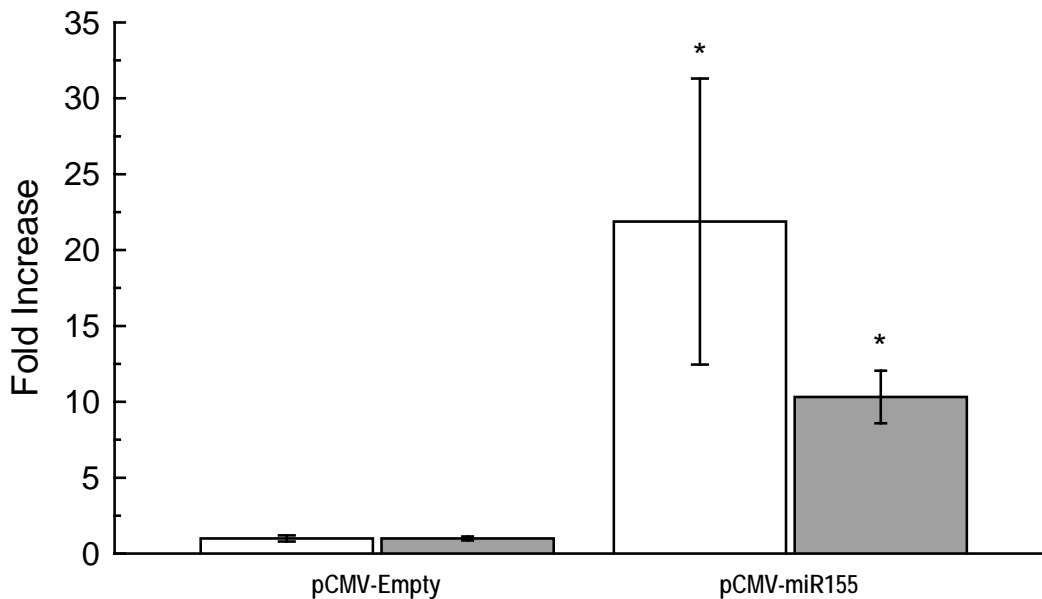


Figure 6. miR-155-5p over-expression by pCMV-miR155 results in increased levels of miR-155-5p and miR-146a-5p measured by qRT-PCR. 1×10^5 J774A.1 macrophages were transfected with Avalanche J774A.1 transfection reagent and pCMV-miR55 or pCMV-Empty vector. 24 hours post-transfection, macrophages were lysed and miRNA was isolated and purified. miR-155-5p (open bars) and miR-146a-5p (grey bars) in pCMV-miR155 transfected cells was 21.9 \pm 9.4 and 10.3 \pm 1.7 fold higher than transfection control cells, respectively ($p < 0.05$). snoRNA U6B was used as a reference transcript to determine the relative fold expression using the $\Delta\Delta C_t$ method, and pCMV-empty group was set equal to 1 for comparison. $n=3$ for all groups. * indicates significance (p -value < 0.05) by t-test. Error bars are standard error of the mean of fold change.

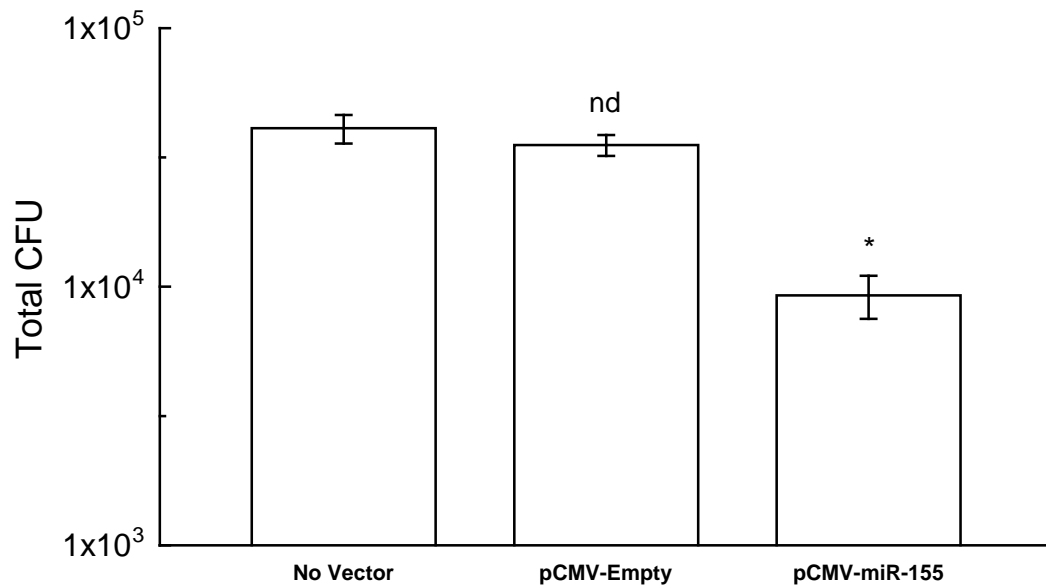


Figure 7. Intracellular levels of *F. novicida* is reduced in cells expressing higher levels of miR-155-5p and miR-146a-5p prior to infection. 24 hours post-transfection, macrophages were infected with stock culture of *F. novicida* U112. At 6 h post-infection, cells transfected with pCMV-miR155 and demonstrating an increase in miR-155-5p and miR-146a-5p displayed a 77.4% reduced intracellular bacterial burden compared to untreated and vector-only control wells. n=3 for all groups. Asterisk indicates significant change ($p < 0.01$) determined by Student's t-test. nd indicates no significant difference compared to control.

In addition to the decrease in total intracellular bacteria in pCMV-miR155 transfected cells, we also measured the effects of the infection on the pre-existing levels of miR-155-5p and miR-146a-5p as determined post-transfection (**Figure 8**). In non-transfected and pCMV-vector controls, the levels of miR-155-5p and miR-146a-5p changed with *F. novicida* infection (**Figure 8**) similarly to what was seen with infection at 72 h (**Figure 4**). However, in the presence of increase miR-155-5p due to over-expression, *F. novicida* infection did further increase miR-155-5p levels. Interestingly, the level of miR-146a-5p was significantly upregulated following *F. novicida* infection of miR-155-5p-transfected cells. This result suggests that the addition of bacterial infection affects miR-146a-5p transcription levels regardless of the over-expression of miR-155-5p, and is in line with its role to fine-tune the release of inflammatory cytokines in response to infection.

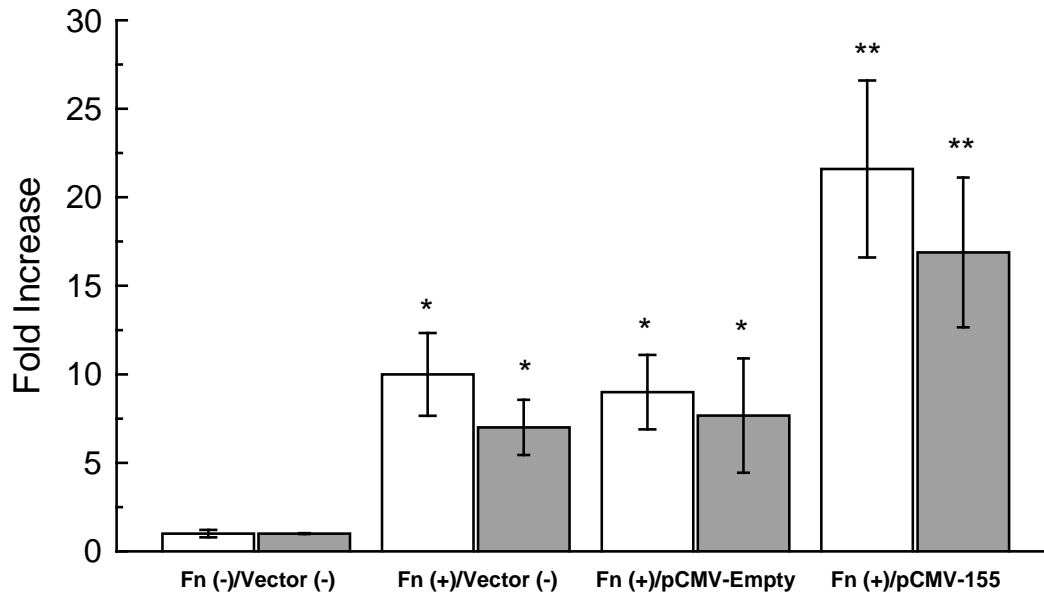


Figure 8. pCMV-miR155 transfected cells infected with *F. novicida* display higher levels of miR-155-5p and miR-146a-5p than non-transfected cells at 6 h post infection. 24 hours post-transfection, macrophages were infected with stock culture of *F. novicida* at an MOI=50. miR-155-5p (open bars) and miR-146a-5p (grey bars) in transfected cells post-infection were 21.6 +/- 5.0 and 16.9 +/- 4.2 -fold higher than non-infected/non-transfected cells, respectively. *F. novicida* infection increased both the miR-155-5p and miR-146a-5p levels in the absence of the pCMV-miR155 expression plasmid at 9.9 +/- 2.3 and 7.7 +/- 3.2-fold, respectively, however no difference was observed between these two groups. n=3 for all groups. * indicates significant increase vs. Fn(-)/Vector(-), ** indicates significant increase vs. all other groups (p -value < 0.05) by t-test. nd indicates no significant difference compared to control. Error bars are standard error of the mean of fold change.

CHAPTER FOUR: DISCUSSION

Pathogens like *F. tularensis* evade host immunity due to their intracellular nature and their ability to disrupt immune responses of the host cell. It has also been shown using other *in vitro* and *in vivo* intracellular pathogen models that intracellular pathogens can affect immune responses of neighboring cells as well- partly through modulation of host exosomes [29, 30]. Since it has been shown that miRNA species in exosomes may represent novel modes of normal signaling among populations of immune cells [34] and that miRNAs are involved in *F. novicida* infection, it was reasonable to hypothesize that an intracellular pathogen like *F. tularensis* could subvert this exosome-signaling system for its own advantage. To begin to address this, the current work examined a tissue culture model of *F. novicida* infection. *F. novicida* infected J774A.1 macrophages showed clear alterations in a number of cellular and exosomal miRNA species when compared to naïve or LPS-treated macrophages, and the over-expression of certain miRNA species in host macrophages had a clear effect on the growth of intracellular *F. novicida*. These data support the hypothesis that the type and amount of miRNAs in exosomes are influenced by *F. novicida* infection and may be factors in disease outcome. These results are presented and discussed with respect to mechanisms of infection as well as from the perspective of identifying novel biomarkers of infection.

The exosomes harvested from naïve, LPS-treated or *F. novicida* infected J774A.1 murine macrophage cell cultures were 50-100 nm in size and displayed the canonical CD63 exosomal membrane marker. Because sequencing studies required large amounts of sample, large fractions of culture medium were collected at 72 h which resulted in fairly large, translucent pellets of exosomes. Although DLS characterization revealed particles larger than those expected for exosomes, as evidenced by the high polydispersion index and increased size distribution plots, exosomes clumping was visualized using electron microscopy. These data are in agreement with previous accounts of exosomes harvested from other cell types (Sokolova *et. al.*) and suggested the exosome fraction from the culture media was successfully separated from the cellular fraction.

The data generated from RNA sequencing experiments suggested a number of specific miRNAs were present in both cells and exosomes with similar abundance despite being infected with live *F. novicida* or purified LPS. These observations are likely due to the specific nature of the miRNAs identified, the lack of interaction between the pathogen and/or pathogen-associated molecular patterns (PAMP). However, a number of the miRNAs appeared differentially expressed between sample types and some miRNAs that appeared upregulated in LPS-treated or infected macrophages have been previously shown to affect cell survival, release of pro-inflammatory cytokines, and down-regulation of pro-apoptotic pathway constituents. Examining all differentially expressed miRNAs in detail was clearly beyond the scope of the current work, but two miRNA transcripts were further examined: miR-155-5p and miR-146a-5p.

Work by others has demonstrated an increase in transcription of miR-155-5p from *F. novicida* infected human monocytes, but no increase in transcription was detected when fully virulent *F. tularensis* was used [19]. In the current work, miR-155-5p appeared upregulated in *F. novicida* infected J774A.1 macrophages as well and also appeared to be increased in exosomes from them. To our knowledge, the increase in exosomal miR-155-5p observed following the infection represents a novel finding. Furthermore, upregulation of exosomal miR-155-5p was not detected when J774A.1 macrophages were treated with *F. tularensis* LVS LPS. Thus, these data may begin to reveal differences between live infections and exposure to bacterial products, and may provide a useful *in vitro* model to begin to study the differences between *F. novicida* and fully virulent strains of *F. tularensis*. In the present work, up-regulation miR-155-5p appears to be maintained out to 72 h post-infection, which could be indicative of downstream pro-survival effects on the phosphorylation of Akt. Although miR-155-5p was not among the 25 most abundantly expressed miRNA transcripts in cell or exosomes, it is clearly important in *F. novicida* infections and results presented herein begin to demonstrate some of the effects of this miRNAs. Indeed, when taken in the context of all of the transcripts from our RNAseq experiments, miR-155-5p represented just under 3% of all of the identified targets. It is unknown if other times points (other than 72 hours) show different expression levels or differential display in exosomes of miR-155-5p, or any other miRNAs but such studies are ongoing.

We also identified high levels of miR-146a-5p (in the list of the top 10 most abundantly expressed miRNAs) in both *F. novicida* infected cells and exosomes from *F.*

novicida infected cells, but no increase was observed in LPS-stimulated macrophages. These also, to our knowledge, represent novel findings. These observations are important because miR-146a-5p has been implicated in adaptive and innate immunity with a variety of disease models. For example, miR-146a-5p targets and degrades IRAK1/2 and TRAF6, both of which are found in close association with MyD88 signaling cascades that can result in Akt and MAPK activation [36]. These targets have been elucidated by molecular means in a variety of studies that stimulated cells with LPS and then monitored the levels of down-stream NF- κ B-driven expression. It is therefore possible that in the macrophage- *F. novicida* model, the negative feedback control by miR-146a-5p over inflammation induced by LPS or infection with *F. novicida* is acting in concert with some of the anti-apoptotic effects that are propagated by increased phosphorylation of Akt resulting from increases in miR-155-5p induced interference with SHIP1. Furthermore, it is possible that this pro-survival signaling strategy may be communicated to naive bystander cells via exosomes, which in turn, down-regulate the inflammatory cytokines released during an infection. Collectively, these results suggest a significant up-regulation in the expression of specific miRNAs in the infected host cell, concomitant with a higher display of specific miRNAs into exosomes, potentially reflecting the infected status of the originating cell. Importantly, it is unclear at this time whether some mechanism exists that differentially packs the various miRNAs into exosomes, but experimental work in this area should be conducted.

Given the increased amount of miR-155-5p in exosomes from *F. novicida* infected cells, it was of interest to begin to examine what consequence this may have on

naïve bystander cells that could potentially take up these exosomes. This would result in more miR-155-5p transcripts than normal in a resting macrophage. For this reason, miR-155-5p was over-expressed in naïve macrophages using the OriGene pCMV-miR based vector system and the transfected cells were infected with *F. novicida*. Results were compared to naïve cells as well as cells transfected with an empty vector. Using a moderate MOI, the results indicated cells expressing higher levels of miR-155-5p prior to infection contain significantly fewer intracellular bacteria 6 hours post-infection. These results are of interest due to the implications it may pose for other relevant *in vitro* infection models.

Interestingly, in addition to the reduced bacterial burden in cells that over-expressed miR-155-5p prior to infection, there was a concomitant increase on the abundance of miR-146a-5p in pCMV-miR-155 transfected cells. These results are in agreement with the known role that miR-146a-5p plays in down-regulating the secretion of pro-inflammatory cytokines in response to increased NF- κ B-based transcription - the down-stream effect of miR-155-5p interaction with SHIP1, which leads to increased NF- κ B signaling through phosphorylated Akt [22]. The levels of miR-146a-5p were further increased 24 hours following infection with *F. novicida*, and add further evidence to support its regulatory role over inflammation in this infection model.

In addition to helping to understand mechanisms of infection, which could lead to better treatment options, the results presented in the current work may also be useful in advancing our ability to diagnose infection. In humans, a diagnosis of tularemia is difficult to make when the route of administration is inhalation. Radiographs are non-

specific and clinical chemistry profiles to date have not been compiled into a single database. Histology can potentially be useful, but reports are generally only made postmortem and findings such as granulomas can be indistinguishable from those seen with miliary tuberculosis lesions that are often seen in the lungs, liver, lymph nodes, and spleen. Some work has been done in animal models. For example, early abscesses have been shown to contain mainly neutrophils, followed later by monocytic cells [31]. Zeidner et al. recently described the pathology of a naturally occurring outbreak of tularemia in prairie dogs where post-mortem examination revealed many pus-filled foci in key organs such as the lungs, liver, and spleen [32], but in general these types of observations require sacrificing the animal. Thus, there is a need to develop better diagnostic methods, including non-invasive methods, in animal models that could ultimately be used in man to diagnose inhalational tularemia. There is a potential for exosomes in this context. Exosomes could be present in granulomas and possibly in the blood or urine of a patient with septic tularemia. It may therefore be possible to develop novel diagnostic methods based on exosomes or their components (e.g., miRNAs) as biomarkers.

Even though the exact mechanism are unknown, it is generally accepted that exosomes and their contents, including exosomal miRNAs, can have significant impacts on a variety of naive host cells such as immune cells responding to a bacterial infection. The work presented here demonstrated the modulatory effects of *F. novicida* infection on the display of miRNAs in infected cells as well as in exosomes released from them. This work also began to address possible consequences of miRNA delivery to naïve bystander

cells by exosomes, effects that may include cell-to-cell signaling and naïve by-stander cell priming. This work also suggested that circulating exosomes may represent novel targets for non-invasive diagnostic methods of *Francisella* infection in animals as well as man.

REFERENCES

1. Morner, T., *The ecology of tularaemia*. Rev Sci Tech, 1992. **11**(4): p. 1123-30.
2. Gallagher-Smith, M., *Francisella tularensis: possible agent in bioterrorism*. Clin Lab Sci, 2004. **17**(1): p. 35-9.
3. McLendon, M.K., M.A. Apicella, and L.A. Allen, *Francisella tularensis: taxonomy, genetics, and Immunopathogenesis of a potential agent of biowarfare*. Annu Rev Microbiol, 2006. **60**: p. 167-85.
4. Stoorvogel, W., et al., *The biogenesis and functions of exosomes*. Traffic, 2002. **3**(5): p. 321-30.
5. Simpson, R.J., et al., *Exosomes: proteomic insights and diagnostic potential*. Expert Rev Proteomics, 2009. **6**(3): p. 267-83.
6. Viaud, S., et al., *Exosomes for the treatment of human malignancies*. Horm Metab Res, 2008. **40**(2): p. 82-8.
7. Clemens, D.L., B.Y. Lee, and M.A. Horwitz, *Virulent and avirulent strains of Francisella tularensis prevent acidification and maturation of their phagosomes and escape into the cytoplasm in human macrophages*. Infect Immun, 2004. **72**(6): p. 3204-17.
8. Craven, R.R., et al., *Francisella tularensis invasion of lung epithelial cells*. Infect Immun, 2008. **76**(7): p. 2833-42.
9. Bradburne, C.E., et al., *Temporal transcriptional response during infection of Type II alveolar epithelial cells with Francisella tularensis LVS supports a general host suppression and bacterial uptake by macropinocytosis*. J Biol Chem, 2013.
10. Celli, J., *Intracellular localization of Brucella abortus and Francisella tularensis in primary murine macrophages*. Methods Mol Biol, 2008. **431**: p. 133-45.

11. Clay, C.D., et al., *Evasion of complement-mediated lysis and complement C3 deposition are regulated by Francisella tularensis lipopolysaccharide O antigen*. J Immunol, 2008. **181**(8): p. 5568-78.
12. Roth, K.M., et al., *Francisella inhibits STAT1-mediated signaling in macrophages and prevents activation of antigen-specific T cells*. Int Immunol, 2009. **21**(1): p. 19-28.
13. Parsa, K.V., et al., *Francisella gains a survival advantage within mononuclear phagocytes by suppressing the host IFN γ response*. Mol Immunol, 2008. **45**(12): p. 3428-37.
14. Telepnev, M., et al., *Francisella tularensis inhibits Toll-like receptor-mediated activation of intracellular signalling and secretion of TNF-alpha and IL-1 from murine macrophages*. Cell Microbiol, 2003. **5**(1): p. 41-51.
15. Katz, J., et al., *Toll-like receptor 2 is required for inflammatory responses to Francisella tularensis LVS*. Infect Immun, 2006. **74**(5): p. 2809-16.
16. Vanhaesebroeck, B., et al., *Phosphoinositide 3-kinases: a conserved family of signal transducers*. Trends Biochem Sci, 1997. **22**(7): p. 267-72.
17. Vanhaesebroeck, B. and D.R. Alessi, *The PI3K-PDK1 connection: more than just a road to PKB*. Biochem J, 2000. **346 Pt 3**: p. 561-76.
18. Helgason, C.D., et al., *A dual role for Src homology 2 domain-containing inositol-5-phosphatase (SHIP) in immunity: aberrant development and enhanced function of b lymphocytes in ship -/- mice*. J Exp Med, 2000. **191**(5): p. 781-94.
19. O'Connell, R.M., et al., *Inositol phosphatase SHIP1 is a primary target of miR-155*. Proc Natl Acad Sci U S A, 2009. **106**(17): p. 7113-8.
20. Cremer, T.J., et al., *MiR-155 induction by F. novicida but not the virulent F. tularensis results in SHIP down-regulation and enhanced pro-inflammatory cytokine response*. PLoS One, 2009. **4**(12): p. e8508.
21. Curtale, G., et al., *An emerging player in the adaptive immune response: microRNA-146a is a modulator of IL-2 expression and activation-induced cell death in T lymphocytes*. Blood, 2009. **115**(2): p. 265-73.
22. Taganov, K.D., et al., *NF-kappaB-dependent induction of microRNA miR-146, an inhibitor targeted to signaling proteins of innate immune responses*. Proc Natl Acad Sci U S A, 2006. **103**(33): p. 12481-6.

23. Perry, M.M., et al., *Divergent intracellular pathways regulate interleukin-1beta-induced miR-146a and miR-146b expression and chemokine release in human alveolar epithelial cells*. FEBS Lett, 2009. **583**(20): p. 3349-55.
24. Jurkin, J., et al., *miR-146a is differentially expressed by myeloid dendritic cell subsets and desensitizes cells to TLR2-dependent activation*. J Immunol, 2010. **184**(9): p. 4955-65.
25. Sokolova, V., et al., *Characterisation of exosomes derived from human cells by nanoparticle tracking analysis and scanning electron microscopy*. Colloids Surf B Biointerfaces, 2011. **87**(1): p. 146-50.
26. Gyorgy, B., et al., *Membrane vesicles, current state-of-the-art: emerging role of extracellular vesicles*. Cell Mol Life Sci, 2011. **68**(16): p. 2667-88.
27. Giri, P.K., et al., *Proteomic analysis identifies highly antigenic proteins in exosomes from M. tuberculosis-infected and culture filtrate protein-treated macrophages*. Proteomics, 2008. **10**(17): p. 3190-202.
28. Giri, P.K. and J.S. Schorey, *Exosomes derived from M. Bovis BCG infected macrophages activate antigen-specific CD4+ and CD8+ T cells in vitro and in vivo*. PLoS One, 2008. **3**(6): p. e2461.
29. Bhatnagar, S., et al., *Exosomes released from macrophages infected with intracellular pathogens stimulate a proinflammatory response in vitro and in vivo*. Blood, 2007. **110**(9): p. 3234-44.
30. Caby, M.P., et al., *Exosomal-like vesicles are present in human blood plasma*. Int Immunol, 2005. **17**(7): p. 879-87.
31. Denzer, K., et al., *Exosome: from internal vesicle of the multivesicular body to intercellular signaling device*. J Cell Sci, 2000. **113 Pt 19**: p. 3365-74.
32. Mraz, M., et al., *MicroRNA isolation and stability in stored RNA samples*. Biochem Biophys Res Commun, 2009. **390**(1): p. 1-4.
33. Hou, J., et al., *MicroRNA-146a feedback inhibits RIG-I-dependent Type I IFN production in macrophages by targeting TRAF6, IRAK1, and IRAK2*. J Immunol, 2009. **183**(3): p. 2150-8.
34. Conlan, J.W., et al., *Mice intradermally-inoculated with the intact lipopolysaccharide, but not the lipid A or O-chain, from Francisella tularensis LVS rapidly acquire varying degrees of enhanced resistance against systemic or*

aerogenic challenge with virulent strains of the pathogen. Microb Pathog, 2003. **34**(1): p. 39-45.

35. Zeidner, N.S., et al., *An outbreak of Francisella tularensis in captive prairie dogs: an immunohistochemical analysis.* Journal Of Veterinary Diagnostic Investigation: Official Publication Of The American Association Of Veterinary Laboratory Diagnosticians, Inc, 2004. **16**(2): p. 150-152.

BIOGRAPHY

Ryan Mackie graduated from Broomfield High School, Broomfield, CO in 1983. She received her Bachelor of Science degree from Colorado State University in 1999. He is currently employed as a Lead Scientist in the Chemical, Biological and Radiological Concepts and Experimentation Branch at the Naval Surface Warfare Center, Dahlgren Division in Dahlgren, VA.